

# AN EMTP-COMPATIBLE PROCEDURE FOR THE EVALUATION OF ELECTROMAGNETIC INDUCED EFFECTS ON POWER NETWORKS

M. D'AMORE M. S. SARTO

Department of Electrical Engineering - University of Rome "La Sapienza"  
Via Eudossiana 18 - 00184 Rome, Italy

## ABSTRACT

A new routine is presented for the calculation of the induced effects on power networks having whatever configuration by using the EMTP. The COUPLING subroutine computes the transient waveforms of the lumped shunt-current sources which are impressed at the port of the network, in order to account for the effects of an incident electromagnetic wave. The subroutine is EMTP-compatible because it utilizes the line-section simulation model computed by the JMARTI subroutine of the EMTP. The obtained transient sources are then defined in the input file of the EMTP. The method presents the advantage of an easy implementation and of an accurate calculation of the coupling simulation model. Applications are carried out in order to predict the induced voltages on medium voltage power networks protected by varistors. Comparisons with the results obtained by a different procedure, which does not use the EMTP, are carried out in order to assess the validity of the proposed approach.

**Keywords:** Coupling, Transient, EMTP, Network.

## 1. INTRODUCTION

The Electromagnetic Transient Program (EMTP) is a widely-used powerful tool for the time-domain analysis of transients in power networks, having whatever configuration, including nonlinear loads [1]. Actually, the EMTP-package is comprehensive of a consistent routine-library, providing accurate simulation models of transmission lines and electrical apparatus.

However, a limitation of the EMTP is related to the difficulty in simulating the coupling phenomena with transient electromagnetic (EM) fields, which often represent severe sources of disturbances in power systems. Therefore, in several cases the design and the optimization of the protection devices against overvoltages cannot leave out of consideration from the EM-coupling mechanism. Several studies have been performed in the past and different models have been proposed in order to evaluate the induced effects of external transient EM-fields on transmission line systems, both in the time- and in the frequency-domain.

An attempt was made in order to implement in the EMTP the calculation of the lightning induced overvoltages [2]. The analysis of the field-excited line-

section was performed by solving the telegraphers' equations in the time-domain by a point-centered finite-difference technique, whereas the task of simulating the other elements in the power system was delivered to the EMTP. The trick of inserting a not-illuminated short lossless line of length  $\Delta l = v\Delta t$  ( $\Delta t$  is the time-step used by the EMTP-code and  $v$  the propagation speed on the short line) was used in order to realize the interfacing with the EMTP. The resulting procedure, referring to single-conductor configurations, is rather complex formally and collects the limitations of the time-domain approaches, such as difficulties in the simulation of frequency-dependent losses, and computation time increasing with the length of the line.

Recently, a combined frequency- and time-domain procedure has been developed for the analysis of field-excited networks with nonlinear loads [3-5]. The method, based on the nodal approach, allows to sum up the advantages of the accurate simulation of the line-sections and the EM-coupling phenomena in the frequency-domain, to the features of the time-domain analysis, suitable for the study of transients in presence of nonlinear devices. The effects of the incident EM-field are represented by means of lumped current sources, which are enforced at the ends of each line-section.

The basic idea of the procedure was then applied to the development of a computer code for the inclusion of the coupling simulation in the EMTP [6]. An external subroutine was set up for the calculation of the transient lumped current sources to define in the input file of the EMTP. However, this subroutine was completely independent of the EMTP with reference to the network simulation model.

In this paper, the new COUPLING subroutine is developed, which is EMTP-compatible because it utilizes the JMARTI subroutine of the EMTP for the simulation of each line-section in the frequency-domain [7,8]. The advantage of the new procedure consists in the reduction of the calculation efforts with respect to the previous method. Moreover, the coupling algorithm and the expressions of the impressed transient current sources come from the analytical treatment of the Maxwell equations, and the interfacing with the EMTP neither require tricks nor approximations.

Applications are carried out to predict the transient voltages and currents induced on overhead medium-

voltage power networks excited by an EMP-plane wave. Comparisons with the results of the procedure described in [5] are performed, in order to assess the efficiency and accuracy of the proposed COUPLING subroutine.

## 2. EQUIVALENT INDUCED SOURCES ON A FIELD-EXCITED POWER NETWORK

Consider a multiconductor power network with  $p$  ports closed on nonlinear loads, above a lossy ground. The network is excited by an external transient EM field.

The linear part of the network is analyzed in the frequency-domain, taking into account the losses and skin-effect in conductors and ground [5]. The EM-coupling to the generic  $j^{\text{th}}$  line-section gives rise to distributed series voltage and shunt current source vectors,  $\mathbf{E}_j(\omega, x)$  and  $\mathbf{J}_j(\omega, x)$ , which can be computed by applying the exact formulation of the curl Maxwell equations. The equivalent circuit of the  $n_j$ -conductor line-section is shown in Fig.1a, in which  $\mathbf{V}_k(\omega)$ ,  $\mathbf{I}_k(\omega)$  and  $\mathbf{V}_j(\omega)$ ,  $\mathbf{I}_j(\omega)$  are the vectors of the wire-to-ground voltages and line currents at the input and output ports, respectively.

The matrix equation relating the input and output quantities of the  $l_j$ -long line-section is expressed in the following form:

$$\begin{bmatrix} \mathbf{V}_k(\omega) \\ \mathbf{I}_k(\omega) \end{bmatrix} = \begin{bmatrix} \Phi_{j11}(\omega, l_j) & \Phi_{j12}(\omega, l_j) \\ \Phi_{j21}(\omega, l_j) & \Phi_{j22}(\omega, l_j) \end{bmatrix} \begin{bmatrix} \mathbf{V}_j(\omega) \\ \mathbf{I}_j(\omega) \end{bmatrix} + \begin{bmatrix} \mathbf{V}_{sj}(\omega) \\ \mathbf{I}_{sj}(\omega) \end{bmatrix} \quad (1)$$

In the previous expression,  $\Phi_{j11}$ ,  $\Phi_{j12}$ ,  $\Phi_{j21}$ ,  $\Phi_{j22}$  are the  $n_j \times n_j$ -matrix coefficients of the transition matrix of the  $j^{\text{th}}$  line-section:

$$\Phi_{j11}(\omega, l_j) = \Phi_{j22}^t(\omega, l_j) = \mathbf{M}_j(\cosh \mathbf{m}_j l_j) \mathbf{M}_j^{-1} \quad (2a)$$

$$\Phi_{j12}(\omega, l_j) = -\mathbf{M}_j(\sinh \mathbf{m}_j l_j) \mathbf{m}_j^{-1} \mathbf{M}_j^{-1} \mathbf{Z}'_j \quad (2b)$$

$$\Phi_{j21}(\omega, l_j) = -\mathbf{Y}'_j \mathbf{M}_j \mathbf{m}_j^{-1} (\sinh \mathbf{m}_j l_j) \mathbf{M}_j^{-1} \quad (2c)$$

in which  $\mathbf{Z}'_j$ ,  $\mathbf{Y}'_j$  are the p.u.l. series impedance and shunt admittance of the line-section, and

$$\mathbf{m}_j = \text{diag}(\lambda_j^{1/2}) \quad (3)$$

$\mathbf{M}_j$  and  $\lambda_j$  being the eigenvector-matrix and the  $j^{\text{th}}$  eigenvalue, respectively, of matrix  $\mathbf{Z}'_j \mathbf{Y}'_j$ .

$\mathbf{V}_{sj}(\omega)$  and  $\mathbf{I}_{sj}(\omega)$  are the lumped series-voltage and shunt-current sources given by the integral expression:

$$\begin{bmatrix} \mathbf{V}_{sj}(\omega) \\ \mathbf{I}_{sj}(\omega) \end{bmatrix} = \int_0^{l_j} \begin{bmatrix} \Phi_{j11}(l_j - x) & \Phi_{j12}(l_j - x) \\ \Phi_{j21}(l_j - x) & \Phi_{j22}(l_j - x) \end{bmatrix} \begin{bmatrix} \mathbf{E}_j(\omega, x) \\ \mathbf{J}_j(\omega, x) \end{bmatrix} dx \quad (4)$$

Notice that only one type of distributed sources should be considered, according to the used coupling model; for instance, if the scattered approach is applied only distributed voltage sources are involved.

Eq.(1) is then rewritten by using the admittance-matrix formulation:

$$\begin{bmatrix} \mathbf{I}_j(\omega) \\ \mathbf{I}_k(\omega) \end{bmatrix} = \begin{bmatrix} \mathbf{Y}_{\pi j} + \mathbf{Y}_{aj} & -\mathbf{Y}_{\pi j} \\ -\mathbf{Y}_{\pi j} & \mathbf{Y}_{\pi j} + \mathbf{Y}_{bj} \end{bmatrix} \begin{bmatrix} \mathbf{V}_j(\omega) \\ \mathbf{V}_k(\omega) \end{bmatrix} + \begin{bmatrix} \mathbf{I}_{sjj}(\omega) \\ \mathbf{I}_{sbj}(\omega) \end{bmatrix} \quad (5)$$

where the admittance matrix coefficients are:

$$\mathbf{Y}_{\pi j}(\omega) = -\Phi_{j12}^{-1}, \quad \mathbf{Y}_{aj}(\omega) = \mathbf{Y}_{bj}(\omega) = \Phi_{j12}^{-1}(\mathbf{1} - \Phi_{j11}) \quad (6a)$$

and the vector of the equivalent shunt-current sources reads:

$$\begin{bmatrix} \mathbf{I}_{sjj}(\omega) \\ \mathbf{I}_{sbj}(\omega) \end{bmatrix} = \begin{bmatrix} \Phi_{j12}^{-1} & \mathbf{0} \\ -\Phi_{j22} \Phi_{j12}^{-1} & \mathbf{1} \end{bmatrix} \begin{bmatrix} \mathbf{V}_{sj}(\omega) \\ \mathbf{I}_{sj}(\omega) \end{bmatrix} \quad (6b)$$

The current-matrix equation (5) is utilized to define the PI-type equivalent circuit of the field-excited line-section shown in Fig.1b. Notice that the shunt-sources are coincident with the terminal short-circuit currents of the field-excited line.

The field-excited network is then represented by enforcing lumped current-sources at the ends of each line-section. The vector  $\mathbf{I}_s(\omega)$  including all the current sources is obtained by inspection of the network:

$$\mathbf{I}_s(\omega) = [\mathbf{I}_{s1}(\omega) \dots \mathbf{I}_{sk}(\omega) \dots \mathbf{I}_{sp}(\omega)]^t \quad (7)$$

The generic  $k^{\text{th}}$  vector coefficient  $\mathbf{I}_{sk}(\omega)$ , representing the impressed current-source at the  $k^{\text{th}}$  port joining  $q_k$  line-sections, is expressed by:

$$\mathbf{I}_{sk}(\omega) = \sum_{j=1}^{q_k} \mathbf{I}_{sa(b)j}(\omega) \quad (8)$$

in which the subscript  $a$  (or  $b$ ) denotes the input (or output) port of the  $j^{\text{th}}$  line-section.

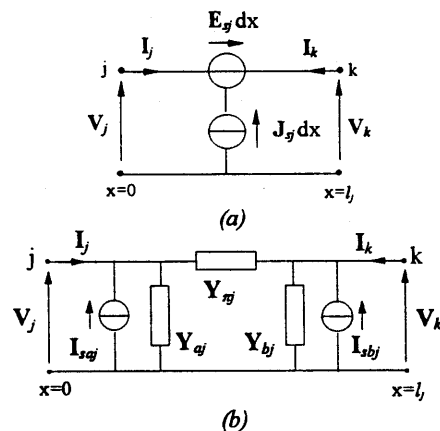


Fig.1 Sketch of the  $j^{\text{th}}$  field-excited multiconductor line-section (a) and PI-type equivalent circuit (b).

In the time-domain, the effect of the EM-coupling is represented by the vector  $\mathbf{i}_s(t)$  of the transient shunt current-sources impressed at the ports of the network, whose coefficients are obtained by inverse Discrete Fourier Transform (DFT) from the frequency-domain:

$$\mathbf{i}_s(t) = F^{-1}[\mathbf{I}_s(\omega)] \quad (9)$$

In a previous paper, an algorithm was implemented to include the simulation of coupling phenomena in the EMTP [6]. An off-line subroutine was used in order to compute the shunt-current sources (6b) at the ends of each line section and the corresponding transient waveforms  $\mathbf{i}_{sq}(t)$ ,  $\mathbf{i}_{sb}(t)$  representing the effects of the impinging EM wave. These sources, which are the coefficients of  $\mathbf{i}_s(t)$ , were considered as impressed current generators exciting the nodes of the network. However, the off-line subroutine for the computation of the shunt-current sources was completely independent of the EMTP and required the evaluation of the whole simulation model of each line section in the frequency-domain.

### 3. THE EMTP-COMPATIBLE PROCEDURE TO SIMULATE THE EM-COUPLING

#### 3.1 The "COUPLING" Subroutine

A procedure is proposed for the calculation of the coefficients of the current source-vector  $\mathbf{i}_s(t)$ , using the line-simulation model computed by the JMARTI subroutine of the EMTP [7,8].

The punched file of the JMARTI subroutine of the EMTP, describing the frequency-domain simulation model of the passive line-section, is utilized as input file of the new subroutine, together with the data describing the source and the geometrical configuration. In the most general case of untransposed multiconductor line-sections, the punched file of the JMARTI subroutine provides the pole-residue approximation of the coefficients of the modal characteristic impedance matrix  $\mathbf{Z}_{cmj}$  and of matrix  $\mathbf{A}_{mj} = \exp(-\mathbf{m}_j l_j)$ , in addition to the coefficients of the current transformation matrix  $\mathbf{N}_j$ .

The output of the JMARTI subroutine is utilized to compute the voltage transformation matrix  $\mathbf{M}_j$ , the diagonal matrix  $\mathbf{m}_j$  and the characteristic impedance and admittance matrices  $\mathbf{Z}_{cj}$  and  $\mathbf{Y}_{cj}$ :

$$\mathbf{M}_j = (\mathbf{N}_j^{-1})^t, \quad \mathbf{m}_j = -(\ln \mathbf{A}_{mj}) l_j^{-1} \quad (10)$$

$$\mathbf{Z}_{cj} = \mathbf{M}_j \mathbf{Z}_{cmj} \mathbf{M}_j^t, \quad \mathbf{Y}_{cj} = \mathbf{N}_j \mathbf{Y}_{cmj} \mathbf{N}_j^t \quad (11)$$

Notice that the transformation matrices  $\mathbf{N}_j$ ,  $\mathbf{M}_j$  are assumed to be frequency-independent in the whole range of interest by the JMARTI subroutine.

Therefore, the matrix coefficients (2a,b,c) of the line transition matrix are expressed in the following form:

$$\Phi_{j11}(\omega, l_j) = \Phi_{j22}(\omega, l_j) = \mathbf{M}_j (\cosh \mathbf{m}_j l_j) \mathbf{N}_j^t \quad (12a)$$

$$\Phi_{j12}(\omega, l_j) = -\mathbf{M}_j (\sinh \mathbf{m}_j l_j) \mathbf{N}_j^t \mathbf{Z}_{cj} \quad (12b)$$

$$\Phi_{j21}(\omega, l_j) = -\mathbf{M}_j \mathbf{Y}_{cj} (\sinh \mathbf{m}_j l_j) \mathbf{N}_j^t \quad (12c)$$

These coefficients are used to obtain the lumped series-voltage and shunt-current sources  $\mathbf{V}_j(\omega)$  and  $\mathbf{I}_j(\omega)$  given by eq.(4) as functions of the known distributed induced sources  $\mathbf{E}_j(\omega, x)$  and  $\mathbf{J}_j(\omega, x)$ . The integral matrix expressions can be computed in general by using a numerical procedure.

Then, the lumped current sources at the ports of the  $j^{\text{th}}$  line-section are computed in the frequency domain by means of eq.(6b) rewritten in following form:

$$\begin{bmatrix} \mathbf{I}_{sq}(\omega) \\ \mathbf{I}_{sb}(\omega) \end{bmatrix} = \begin{bmatrix} -\mathbf{Y}_{cj} \mathbf{M}_j (\sinh^{-1} \mathbf{m}_j l_j) \mathbf{N}_j^t & 0 \\ \mathbf{N}_j (\cotgh \mathbf{m}_j l_j) \mathbf{M}_j^t \mathbf{Y}_{cj} & \mathbf{U} \end{bmatrix} \begin{bmatrix} \mathbf{V}_j(\omega) \\ \mathbf{I}_j(\omega) \end{bmatrix} \quad (13)$$

Finally,  $\mathbf{I}_s(\omega)$  is computed by using eq.(7), and the vector of the transient current sources  $\mathbf{i}_s(t)$  is obtained by applying the inverse DFT. The output file of the off-line subroutine supplies the values of the coefficients of the transient source vector  $\mathbf{i}_s(t)$  at each time step, and is considered as the part of the input file of the EMTP defining the excitation of the network.

Actually, the coefficients of vector  $\mathbf{i}_s(t)$  are defined in the input file of the PC-version of the EMTP as *static empirical sources* [1]; the *Type-1 source definition card* is introduced after the blank card ending the switches, whereas the grouping of *Type-1 function value specification cards*, constituted by the output of the off-line subroutine, follows the card ending requests for program outputs. The structure of the input file of the EMTP for the transient analysis of a field-excited network is sketched in Table I. The flow graph of the EMTP-compatible procedure is shown in Fig. 2

TABLE I

Sketch of the input file of the EMTP for the transient analysis of a field-excited network.

Cards to begin a new data case									
Cards for linear and nonlinear branches									
BLANK card ending electrical network branches									
Cards for electric-network switches, diodes ...									
BLANK card ending switches									
Source cards for electric network									
	1	2	3	4	5	6	7	8	9 10
	1		name of the excited node						- 1
	1		....						- 1
BLANK card ending electric network source cards									
Node voltage output specification card									
BLANK card ending output specification cards									
Cards for specifying Type-1 source function									
End									

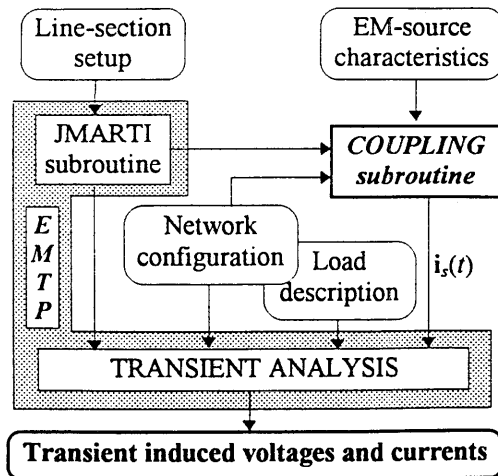


Fig. 2 Flow graph of the procedure for the calculation of the EM induced effects on a power network by the EMTP.

### 3.2 Exciting Sources Induced by a Plane Wave

In case the network is excited by a plane wave having incidence and azimuth angles  $\vartheta$  and  $\psi$  respectively (Fig.3), the distributed induced sources  $E_j(\omega, x)$ ,  $J_j(\omega, x)$  are defined by an accurate coupling model which takes into account the reflection from the lossy ground [5].

The integral expressions (4) of the sources  $V_j(\omega)$ ,  $I_j(\omega)$  are resolved analytically and the following matrix formulation is obtained:

$$\begin{bmatrix} V_j(\omega) \\ I_j(\omega) \end{bmatrix} = \frac{1}{2} \begin{bmatrix} -U & Z_{cj} \\ Y_{cj} & -U \end{bmatrix} \begin{bmatrix} P_{Mj}^+ Q_{Mj}^+ R_{Mj}^- & 0 \\ 0 & P_{Nj}^+ Q_{Nj}^+ R_{Nj}^- \end{bmatrix} + \begin{bmatrix} U & Z_{cj} \\ Y_{cj} & U \end{bmatrix} \begin{bmatrix} P_{Mj}^- Q_{Mj}^- R_{Mj}^+ & 0 \\ 0 & P_{Nj}^- Q_{Nj}^- R_{Nj}^+ \end{bmatrix} \begin{bmatrix} E_j(\omega, 0) \\ J_j(\omega, 0) \end{bmatrix} \quad (14)$$

in which  $U$  is the unit-matrix,  $E_j(\omega, 0)$  and  $J_j(\omega, 0)$  are the distributed sources computed at the input port  $x_j=0$  of the  $j^{\text{th}}$  line-section, and:

$$P_{Mj}^{\pm} = M_j \left[ \exp(\pm m_j l_j) \right] M_j^{-1} \quad (15a)$$

$$P_{Nj}^{\pm} = N_j \left[ \exp(\pm m_j l_j) \right] N_j^{-1} \quad (15b)$$

$$Q_{Mj}^{\pm} = \left[ M_j m_j M_j^{-1} \pm j k_0 \cos \vartheta \cos \psi U \right]^{-1} \quad (15c)$$

$$Q_{Nj}^{\pm} = \left[ N_j m_j N_j^{-1} \pm j k_0 \cos \vartheta \cos \psi U \right]^{-1} \quad (15d)$$

$$R_{Mj}^{\pm} = \left[ \exp(-k_0 \cos \vartheta \cos \psi l_j) \right] P_{Mj}^{\pm} - U \quad (15e)$$

$$R_{Nj}^{\pm} = \left[ \exp(-k_0 \cos \vartheta \cos \psi l_j) \right] P_{Nj}^{\pm} - U \quad (15f)$$

with  $k_0 = \omega(\epsilon_0 \mu_0)^{1/2}$ .

The obtained analytical expressions (14) are utilized in eq.(13) for a fast computation of the lumped induced current sources.

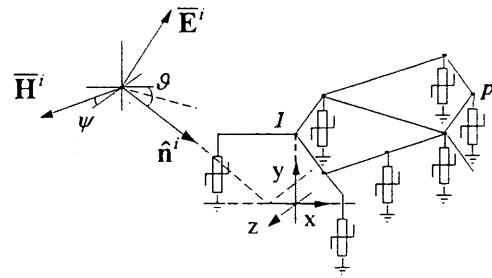


Fig.3 Sketch of a multiconductor network illuminated by an EM-plane wave.

## 4. APPLICATIONS

The COUPLING subroutine is used for the transient analysis of medium-voltage (MV) power networks, illuminated by an EMP-plane wave having incidence and azimuth angles  $\vartheta=50^\circ$  and  $\psi=20^\circ$ , respectively. The electric field is represented in the time-domain by a double exponential function having amplitude of 50 kV/m, and time constants  $\tau_1=150$  ns and  $\tau_2=2$  ns. The ground resistivity and relative permittivity are equal to  $10 \Omega/m$  and 1, respectively.

In the first application, the untransposed multiconductor line sketched in Fig.4a is considered. The line-section has the geometrical configuration shown in Fig.4b. The terminal loads are constituted by MV/LV transformers parallel connected to  $500 \Omega$  resistances, and protected by ZnO-varistors having threshold voltage of 24 kV. The corona phenomenon is neglected in the line-model.

The data describing the line-setup are used in the input file of the JMARTI subroutine; the punched file of the EMTP subroutine, the characteristics of the EM-source and the geometrical configuration of the system are then used as input of the COUPLING subroutine, which provides the current source vector  $i_s(t)$  in the time-domain. Fig.5 shows the computed waveforms of the sources impressed on conductor 1 at the near and far end of the line. It has already been observed that  $i_{sa}(t)$  and  $i_{sb}(t)$  are coincident with the vectors of the terminal short-circuit current; therefore, the curves in Fig. 5 are characterized by several peaks, which represent the reflections of the current traveling waves at the ends of the line.

Successively, the computed transient sources are included in the input file of the EMTP for the time-domain analysis, following the sketch in Table I. The MV/LV transformers are represented in the high frequency-range by phase-to-ground capacitances  $C=1$  nF, and the varistors by the dynamic nonlinear simulation model, including the effects of the stray inductance  $L_v=1 \mu H$  and the parasitic capacitance  $C_v=20$  pF [6]. The waveforms of the induced voltages on conductor 1 at the near and far ends are computed by using the proposed EMTP-compatible procedure (Fig.6a) and the method developed in [5] (Fig.6b).

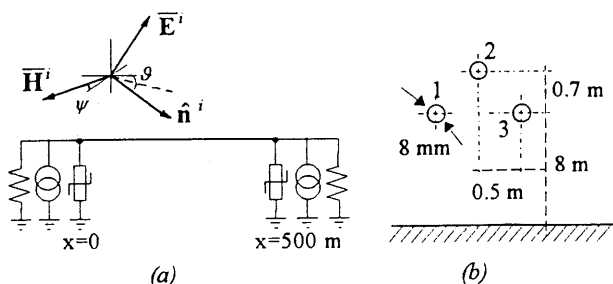


Fig.4 Sketch (a) and geometrical configuration (b) of a multiconductor field-excited line.

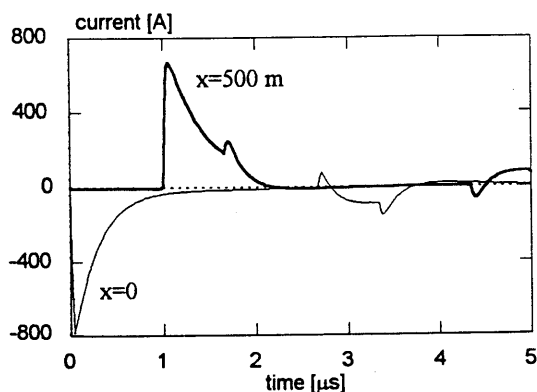


Fig. 5 Transient waveforms of the induced shunt current sources on conductor 1 at  $x=0$  (—) and  $x=500$  m (---).

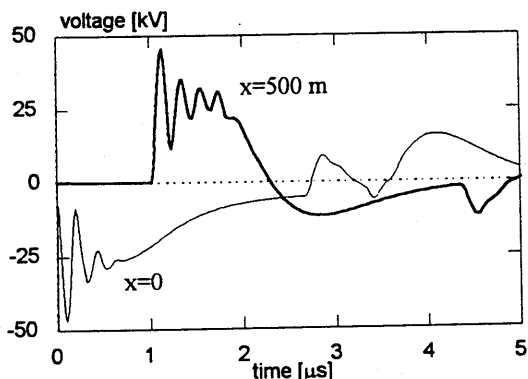
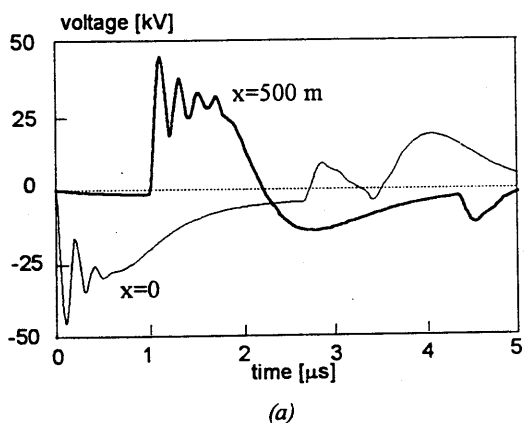


Fig.6 Induced voltages on wire 1 at  $x=0$  (—) and  $x=500$  m (---) computed by using the COUPLING subroutine (a) and a different procedure [5] (b).

The results of the two approaches are in good agreement. The differences in the waveforms give

evidence that in the method described in [5] the exact simulation model of the line is used, whereas in the JMARTI subroutine the transformation matrices are assumed to be constant in the whole frequency range of interest.

In the second application, the MV network shown in Fig.7 is considered. The terminal loads are assumed to be the same as in the previous calculation. The network has four ports, and three line-sections constituted by three parallel wires, as shown in Fig.4b; therefore, twelve shunt-current sources have to be enforced at the ends of the line-sections in order to compute the induced effects by the external EM-field.

The waveforms of the impressed current sources on conductor 1 at ports 3 and 4 are shown in Fig.8. The multiple peaks account for the reflections of the current waves at the ports of the network. With reference to the waveform of the current source at port 3 (—), it is interesting to notice that the first peak occurs after the time-delay of the EM-wave propagating in free space, from port 1 to port 3. The second peak represents the current wave which is impressed at port 1 and after traveling along the line-section 1-3 reaches port 3; therefore, it is delayed with respect to the first peak, because the length of the path to cover is defined by the geometrical configuration of the network.

The induced voltages at the same nodes, computed by using the proposed EMTP-procedure and the method described in [5], are then reported in Figs.9a and 9b, respectively. In this case the MV/LV transformers are represented by the phase-to-ground capacitance  $C=1$  nF, whereas the static simulation model of the varistors is considered. The obtained results are still in good agreement, mainly at the beginning of the transient. In fact, after the early 5 micro-seconds, it can be noticed that the waveforms obtained by the EMTP are characterized by greater amplitude than the curves in Fig.9b. Actually, the effects of the frequency-dependent losses of the line are more important after several reflections of the traveling voltage and current waves along the network.

## 5. CONCLUSIONS

The proposed formulation of the EM-coupling model allows to analyze transients in field-excited networks by using the EMTP in a very efficient way, with reference to both transposed and untransposed multiconductor line-sections.

The EM-coupling of an external transient field to the branches of a power network gives rise to distributed series-voltages and shunt-current sources which are supposed to be known in the frequency-domain. Of course, it is possible to consider other types of distributed sources, depending on the considered coupling model. The distributed induced sources are

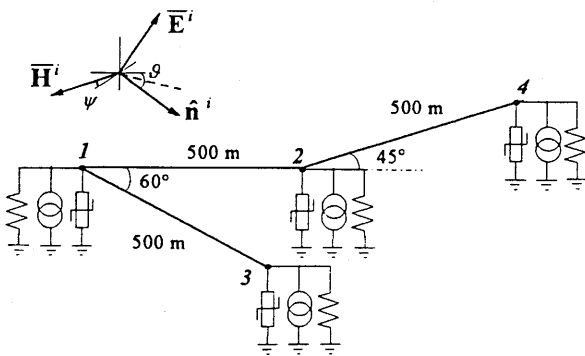


Fig. 7 Sketch of the field-excited multiconductor network.

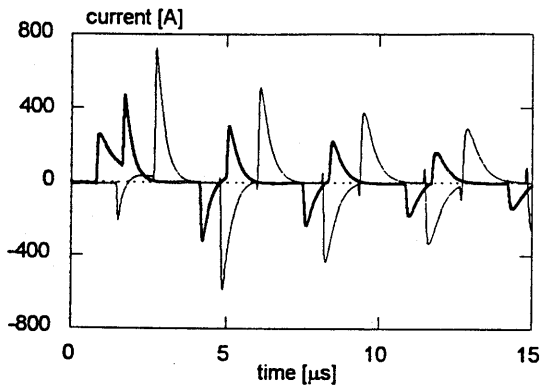


Fig. 8 Transient waveforms of the impressed shunt-current sources on conductor 1 at port 3 (—) and port 4 (---) of the network in Fig. 7.

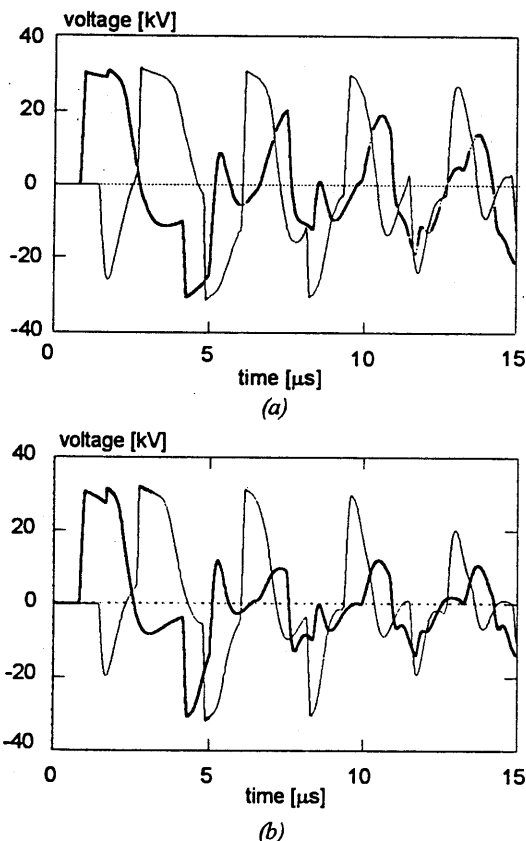


Fig. 9 Induced voltages on wire 1 at port 3 (—) and port 4 (---), by using the COUPLING subroutine (a) and a different procedure [5] (b).

utilized by the COUPLING subroutine to compute the equivalent lumped sources impressed at both the ends of each line section.

The proposed subroutine is EMTP-compatible because it makes use of the JMARTI subroutine of the EMTP for the simulation of multiconductor line-sections in the frequency-domain. The inverse Discrete Fourier Transform is applied to the coefficients of the shunt-current source vector in order to compute the transient waveforms of the generators which are enforced at each port of the network for the transient analysis by the EMTP. The computed induced voltages at the ports of medium-voltage power networks illuminated by an EMP-plane wave are very close to the ones obtained by means of a different code previously developed.

Advantages of the method are the easy interfacing between the COUPLING subroutine and the EMTP as well as the high accuracy of the coupling simulation model, basing on a frequency-domain formulation.

The procedure should be improved by using the new model for the simulation of a poor conducting ground in a wide frequency-range, instead of the Carson's approximated formulation. Moreover, a nonlinear model accounting for the corona phenomenon will be developed.

## 6. REFERENCES

- [1] Alternative Transient Program Rule Book, Leuven EMTP Center (LEC), July, 1987.
- [2] C. A. Nucci, V. Bardazzi, R. Iorio, A. Mansaldo, A. Porrino, "A code for the calculation of lightning-induced overvoltages and its interface with the Electromagnetic Transient Program", 22<sup>nd</sup> International Conference on Lightning Protection, Budapest, 1994.
- [3] M. D'Amore, M. S. Sarto, "EMP-coupling to multiconductor dissipative lines with nonlinear loads above a lossy ground", Proc. 10<sup>th</sup> Zurich Symp. on EMC, Zurich, March 9-11, 1993.
- [4] M. D'Amore, M. S. Sarto, "EMP induced effects on power lines protected by surge arresters", Proc. CIGRÉ Conference on Power System EMC, Lausanne, October 18-20, 1993.
- [5] M. D'Amore, M. S. Sarto, "Time-response of a network containing field-excited multiconductor lossy lines with nonlinear loads", Proc. 1993 IEEE EMC Int. Symp., Dallas, August 9-13, 1993.
- [6] M. D'Amore, M. S. Sarto, "A new efficient procedure for the transient analysis of dissipative power networks with nonlinear loads", IEEE 1995 Power Summer Meeting, Portland, OR, 23-17 July, 1995.
- [7] J. R. Marti, "Accurate modelling of frequency-dependent transmission lines in electromagnetic transient simulations", IEEE Trans. on PAS, Vol. PAS-101, No. 1, Jan. 1982, pp.147-155.
- [8] J. R. Marti, "Simulation of transients in underground cables with frequency-dependent modal transformation matrices", IEEE Trans. on PWDR, Vol. 3, No.3, July 1988, pp.1099-1110.